

HINTS OF DYNAMICAL VACUUM ENERGY IN THE EXPANDING UNIVERSE

JOAN SOLÀ^{1,2}, ADRIÀ GÓMEZ-VALENT^{1,2}, AND JAVIER DE CRUZ PÉREZ¹¹ High Energy Physics Group, Dept. ECM, Univ. de Barcelona, Av. Diagonal 647, E-08028 Barcelona, Catalonia, Spain;

sola@ecm.ub.edu, adriagova@ecm.ub.edu, jdcrupe7@alumnes.ub.edu

² Institut de Ciències del Cosmos (ICC), Univ. de Barcelona, Av. Diagonal 647, E-08028 Barcelona, Catalonia, Spain

Received 2015 July 16; accepted 2015 September 2; published 2015 September 22

ABSTRACT

Recently there have been claims of model-independent evidence of dynamical dark energy. Herein we consider a fairly general class of cosmological models with a time-evolving cosmological term of the form $\Lambda(H) = C_0 + C_H H^2 + C_{\dot{H}} \dot{H}$, where H is the Hubble rate. These models are well motivated from the theoretical point of view since they can be related to the general form of the effective action of quantum field theory in curved spacetime. Consistency with matter conservation can be achieved by letting the Newtonian coupling G change very slowly with the expansion. We solve these dynamical vacuum models and fit them to the wealth of expansion history and linear structure formation data. The results of our analysis indicate a significantly better agreement as compared to the concordance Λ CDM model, thus supporting the possibility of a dynamical cosmic vacuum.

Key words: cosmology: observations – dark energy – large-scale structure of universe – methods: numerical – methods: statistical

1. INTRODUCTION

The positive evidence that our universe is speeding up owing to some form of dark energy (DE) pervading all corners of interstellar space seems to be, nowadays, beyond doubt after the first measurements of distant supernovae (Riess et al. 1998; Perlmutter et al. 1999) and the most recent analysis of the precision cosmological data by the Planck Collaboration (Ade et al. 2015). The ultimate origin of such a positive acceleration is unknown, but the simplest possibility would be the presence of a tiny and positive cosmological constant (CC) in Einstein’s field equations, $\Lambda > 0$. This framework, the so-called concordance or Λ CDM model, seems to describe quite well the observations (Ade et al. 2015) but, unfortunately, there is little theoretical motivation for it. The CC is usually associated with the energy density carried by the vacuum through the parameter $\rho_\Lambda = \Lambda/(8\pi G)$ (in which G is the Newtonian coupling), although it is difficult to reconcile its measured value ($\rho_\Lambda \sim 10^{-47} \text{ GeV}^4$) with typical expectations in quantum field theory (QFT) and string theory, which are many orders of magnitude bigger. Such a situation has been triggered in the past—only to find it reinforced at present—the old CC problem and the cosmic coincidence problem (Weinberg 1989; Sahni & Starobinsky 2000; Padmanabhan 2003; Peebles & Ratra 2003), both of which lie at the forefront of fundamental physics.

Different theoretical scenarios have been proposed for quite some time. In this Letter we take seriously the recent observational hint that the DE could be dynamical as a means to alleviate some tensions recently observed with the Λ CDM (Sahni et al. 2014). Specifically, we focus on the dynamical vacuum models of the form $\Lambda(H) = C_0 + C_H H^2 + C_{\dot{H}} \dot{H}$, in which $H = \dot{a}/a$ and $\dot{H} = dH/dt$ are the Hubble rate and its cosmic time derivative, with $C_0 \neq 0$ a constant. We assume that at least one of the coefficients C_H and $C_{\dot{H}}$ is nonvanishing. Such models possess a well-defined Λ CDM limit ($C_H, C_{\dot{H}} \rightarrow 0$) and involve two time derivatives of the scale factor, and therefore can be consistent with the general covariance of the effective action of QFT in curved spacetime. While the general structure of $\Lambda(H)$ can be conceived as an

educated phenomenological ansatz, it can actually be related to the quantum effects on the effective vacuum action due to the expanding background, in which the leading effects may generically be captured from a renormalization group equation (Solà 2008, 2013, 2015; Shapiro & Solà 2009; Solà & Gómez-Valent 2015). The dimensionless coefficients C_H and $C_{\dot{H}}$ are actually related to the β -function of the running and are therefore naturally small. In the presence of matter conservation, this is possible by letting $G = G(H)$ be dynamical as well (Solà 2008, 2013). A generalization of $\rho_\Lambda(H)$ with higher powers of the Hubble rate, i.e., H^n ($n > 2$), has been recently used to describe inflation (see, e.g., Lima et al. 2013; Solà 2015).

In the following we solve these dynamical vacuum models $\Lambda(H)$ and test them in light of recent observational data, and compare their performance with the concordance Λ CDM model.

2. BACKGROUND COSMOLOGICAL SOLUTIONS

The field equations for the dynamical vacuum energy density in the Friedmann–Lemaître–Robertson–Walker (FLRW) metric in flat space are derived in the standard way and are formally similar to the ones with strictly constant G and Λ terms:

$$3H^2 = 8\pi G(H)(\rho_m + \rho_r + \rho_\Lambda(H)) \quad (1)$$

$$3H^2 + 2\dot{H} = -8\pi G(H)(p_\Lambda(H) + p_r), \quad (2)$$

where $\rho_\Lambda(H) = \Lambda(H)/(8\pi G(H))$ is the dynamical vacuum energy density, $p_\Lambda(H) = -\rho_\Lambda(H)$, and $G(H)$ is the dynamical gravitational coupling. It is convenient to take into account the effect of relativistic matter, i.e., $p_r = (1/3)\rho_r$, together with dust ($p_m = 0$) from the beginning. We consider the following two realizations of the dynamical vacuum model:

$$G1: \quad \Lambda(H) = 3(c_0 + \nu H^2) \quad (3)$$

$$G2: \quad \Lambda(H, \dot{H}) = 3\left(c_0 + \nu H^2 + \frac{2}{3}\alpha \dot{H}\right), \quad (4)$$

where we have redefined $C_0 = 3c_0$, $C_H = 3\nu$, and $C_{\dot{H}} = 2\alpha$ for convenience. Model G1 is, of course, a particular case of Model G2, but it will be useful to distinguish between them. We can combine (1) and (2) to obtain the equation of local covariant conservation of the energy, i.e. $\nabla^\mu(GT_{\mu 0}) = 0$. Explicitly, since we assume matter conservation (meaning $\dot{\rho}_m + 3H\rho_m = 0$ and $\dot{\rho}_r + 4H\rho_r = 0$), it leads to a dynamical interplay between the vacuum and the Newtonian coupling:

$$\dot{G}(\rho_m + \rho_r + \rho_\Lambda) + G\dot{\rho}_\Lambda = 0. \quad (5)$$

Trading the cosmic time for the scale factor a , the previous equations amount to determine G as a function of a . Using the matter conservation equations, we arrive at

$$G(a) = -G_0 \left[\frac{a(E^2(a))'}{3\Omega_m a^{-3} + 4\Omega_r a^{-4}} \right], \quad (6)$$

where $G_0 \equiv G(a=1)$ is the present value of G , and $E(a) = H(a)/H_0$ is the normalized Hubble rate to its present value. The prime stands for d/da , and $\Omega_i = \rho_{i0}/\rho_{c0}$ (with $\rho_{c0} = 3H_0^2/8\pi G_0$) is the currently normalized energy density with respect to the critical density. Inserting (4) and the above result for $G(a)$ in Equation (1) and integrating, we obtain:

$$E^2(a) = 1 + \frac{\Omega_m}{\xi} \left[-1 + a^{-4\xi'} \left(a + \frac{\xi \Omega_r}{\xi' \Omega_m} \right)^{\frac{\xi'}{1-\alpha}} \right], \quad (7)$$

where we have introduced

$$\xi = \frac{1-\nu}{1-\alpha} \equiv 1 - \nu_{\text{eff}}, \quad \xi' = \frac{1-\nu}{1-\frac{4}{3}\alpha} \equiv 1 - \nu'_{\text{eff}}. \quad (8)$$

For small $|\nu, \alpha| \ll 1$ (the expected situation), we can use the approximations $\nu_{\text{eff}} \simeq \nu - \alpha$ and $\nu'_{\text{eff}} \simeq \nu - (4/3)\alpha$. Note that, in order to simplify the presentation, we have removed terms proportional to $\Omega_r \ll \Omega_m$ from Equation (7) that are not relevant here. We can check, e.g., that in the radiation-dominated epoch the leading term in the expression (7) is $\sim \Omega_r a^{-4\xi'}$, while it is $\sim \Omega_m a^{-3\xi}$ in the matter-dominated epoch. Furthermore, we find that the (full) expression for $E^2(a)$ reduces to the Λ CDM form, $1 + \Omega_m(a^{-3} - 1) + \Omega_r(a^{-4} - 1)$, in the limit $\nu, \alpha \rightarrow 0$ (i.e., $\xi, \xi' \rightarrow 1$). Note also the constraint among the parameters, $c_0 = H_0^2 \left[\Omega_\Lambda - \nu + \alpha \left(\Omega_m + \frac{4}{3} \Omega_r \right) \right]$, which follows from matching the vacuum energy density $\rho_\Lambda(H)$ to its present value ρ_Λ^0 for $H = H_0$ and using $\Omega_m + \Omega_r + \Omega_\Lambda = 1$. The explicit scale factor dependence of the Newtonian coupling ensues upon inserting (7) in (6) and computing the derivative. We refrain once more from writing out the full expression here, but one can check that in the limit $a \rightarrow 0$ (relevant for the Big Bang Nucleosynthesis epoch) it behaves as

$$G(a) = G_0 a^{4(1-\xi')} \simeq G_0 (1 + 4\nu'_{\text{eff}} \ln a). \quad (9)$$

Thus, the gravitational coupling evolves logarithmically with the scale factor and hence changes very slowly. This logarithmic law was motivated previously by Solà (2008, 2013) within the context of the renormalization group of QFT

in curved spacetime. For $\nu = \alpha = 0$ we obtain $G = G_0$ identically, i.e., the current value of the gravitational coupling. However the situation $G = G_0$ is also attained in the limit $a \rightarrow 0$ for $\nu = (4/3)\alpha$ (i.e., $\xi' = 1$); and indeed we shall adopt this setting hereafter in order to maximally preserve the BBN constraint for the G2 model. The effective fitting parameter will be $\nu_{\text{eff}} = \nu/4$. Obviously this setting is impossible for G1, so in this case we will adopt the average BBN restriction $|\Delta G/G| < 10\%$ used in the literature (Chiba 2011; Uzan 2011). At the same time we require $|\Delta G/G| < 5\%$ at recombination ($z \simeq 1100$) for both G1 and G2 from the cosmic microwave background (CMB) anisotropy spectrum (Chiba 2011).

The expression for the dynamical vacuum energy density can be obtained from Friedmann's Equation (1), in combination with the explicit form of $G(a)$. We quote here only the simplified expression valid for the matter-dominated epoch:

$$\rho_\Lambda(a) = \rho_{c0} a^{-3} \left[a^{3\xi} + \frac{\Omega_m}{\xi} (1 - \xi - a^{3\xi}) \right]. \quad (10)$$

For $\xi \rightarrow 1$ we have $\rho_\Lambda \rightarrow \rho_{c0}(1 - \Omega_m) = \rho_{c0}\Omega_\Lambda$ and we retrieve the Λ CDM case with strictly constant ρ_Λ . The form (10) is sufficient to obtain an effective DE density $\rho_D(z)$ and effective equation of state (EoS) for the DE at fixed $G = G_0$, as is conventionally used in different places of the literature (see, e.g., Solà & Stefancic 2006; Shafieloo et al. 2006; Basilakos & Solà 2014). We find

$$\omega_D(a) = - \frac{1}{1 + \frac{\rho_m(a) G(a) - G_0}{\rho_\Lambda(a) G(a)}}. \quad (11)$$

In Figure 1 (left) we plot ω_D as a function of the cosmic redshift $z = -1 + 1/a$ for models G1 and G2. Near our time, ω_D stays very close to -1 (compatible with the Λ CDM), but at high z it departs. In the same Figure 1 (right) we plot $\Omega_D(z) = \rho_D(z)/\rho_c(z)$, i.e., the normalized DE density with respect to the critical density at constant G_0 . The asymptotes of ω_D for each model at $z > 4$ are due to the vanishing of $\Omega_D(z)$ at the corresponding point (as clearly seen in the figure)—confer the aforementioned references for similar features.

3. FITTING THE MODELS TO THE OBSERVATIONAL DATA

Let us now test these models against observations. First of all, we use the available measurements of the Hubble function as collected in Ding et al. (2015). These are essentially the data points of Farooq & Ratra (2013) in the redshift range $0 \leq z \leq 1.75$ and the baryonic acoustic oscillation (BAO) measurement at the largest redshift $H(z=2.34)$ taken after Delubac et al. (2015) on the basis of BAOs in the Ly α forest of BOSS DR11 quasars. We define the following χ^2 function, to be minimized:

$$\chi_{\text{Omh}^2}^2 = \sum_{i=1}^{N-1} \sum_{j=i+1}^N \left[\frac{\text{Omh}_{\text{th}}^2(H_i, H_j) - \text{Omh}_{\text{obs}}^2(H_i, H_j)}{\sigma_{\text{Omh}^2 ij}} \right]^2, \quad (12)$$

where N is the number of points $H(z)$ contained in the data set, $H_i \equiv H(z_i)$, and the two-point diagnostic $\text{Omh}^2(z_2, z_1) \equiv [h^2(z_2) - h^2(z_1)] / [(1+z_2)^3 - (1+z_1)^3]$

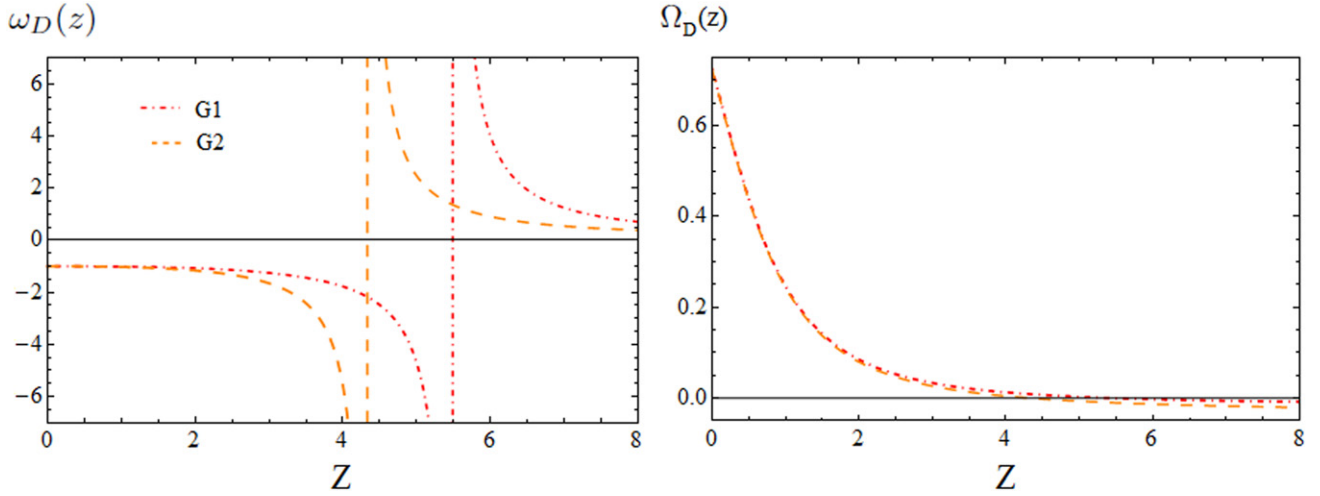


Figure 1. Left: evolution of the effective EoS $\omega_D(z)$, Equation (11), for the models under consideration: Right: the corresponding evolution of the effective DE density $\Omega_D(z)$ normalized to the critical density (see text).

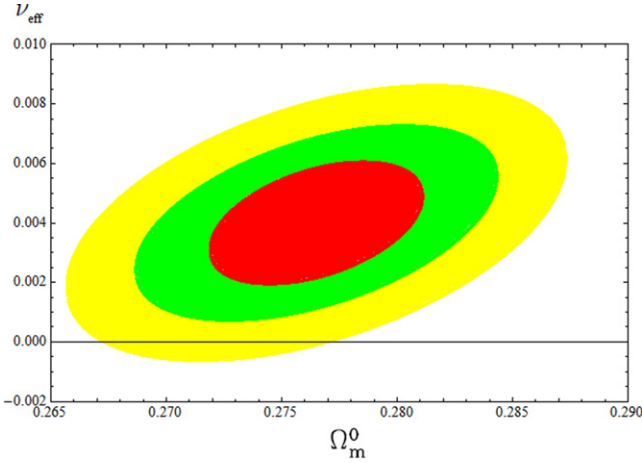


Figure 2. Likelihood contours in the $(\Omega_m, \nu_{\text{eff}})$ plane (for the values $-2 \ln \mathcal{L}/\mathcal{L}_{\text{max}} = 2.30, 6.16, 11.81$, corresponding to $1\sigma, 2\sigma$, and 3σ confidence levels for the G2 model using the full data analysis indicated in Table 2. The $\nu_{\text{eff}} = 0$ region (Λ CDM) is disfavored at $\sim 3\sigma$.

was defined in Sahni et al. (2014), with $h(z) = h E(z)$, and $\sigma_{\text{Om}h^2_{i,j}}$ is the uncertainty associated to the observed value $\text{Om}h^2_{\text{obs}}(H_i, H_j)$ for a given pair of points ij , viz.

$$\sigma_{\text{Om}h^2_{i,j}}^2 = \frac{4 \left[h^2(z_i) \sigma_{h(z_i)}^2 + h^2(z_j) \sigma_{h(z_j)}^2 \right]}{\left[(1+z_i)^3 - (1+z_j)^3 \right]^2}. \quad (13)$$

For Λ CDM, the two-point diagnostic boils down to $\text{Om}h^2(z_2, z_1) = \Omega_m h^2$, which is constant for any pair z_1, z_2 . Using this testing tool and the known observational information on $H(z)$ at the three redshift values $z = 0, 0.57$, and 2.34 , the aforementioned authors observed that the average result is: $\text{Om}h^2 = 0.122 \pm 0.010$, with very little variation from any pair of points taken. The obtained result is significantly smaller than the corresponding Planck value of the two-point diagnostic, which is constant and given by $\text{Om}h^2 = \Omega_m h^2 = 0.1415 \pm 0.0019$ (Ade et al. 2015).

A departure of $\text{Om}h^2$ from the Planck result should, according to Sahni et al. (2014), signal that the DE cannot be

described by a rigid CC. For the Λ CDM we obtain $\text{Om}h^2 = 0.1250 \pm 0.0039$, and $\text{Om}h^2 = 0.1402 \pm 0.0059$, by taking all data points and excluding the high-redshift one, respectively. Since there is a priori no reason to exclude the high-redshift point (Delubac et al. 2015), whose uncertainty is one of the lowest in the full data sample, relaxing the tension with data may require the dynamical nature of the DE. For the vacuum models G1 and G2 considered here, Equations (3) and (4), aim at cooperating in this task.

For these models the theoretical value $\text{Om}h^2_{\text{th}}$ of the two-point diagnostic entering (12) can be computed, in the matter-dominated epoch (relevant for such observable), as follows:

$$\text{Om}h^2_G(z_i, z_j) = \frac{\Omega_m h^2 \left((1+z_i)^{3\xi} - (1+z_j)^{3\xi} \right)}{\xi \left[(1+z_i)^3 - (1+z_j)^3 \right]}. \quad (14)$$

It is evident that for $\xi = 1$ we recover the Λ CDM result, which remains anchored at $\text{Om}h^2(z_i, z_j) = \Omega_m h^2$ ($\forall z_i, \forall z_j$). However, when we allow some small vacuum dynamics (meaning ν and/or α different from zero) we obtain a small departure of ξ from 1 and therefore the DE diagnostic $\text{Om}h^2$ deviates from $\Omega_m h^2$. In this case, $\text{Om}h^2$ evolves with cosmic time (or redshift).

To the above Hubble parameter data we add the recent supernovae type Ia data (SN Ia), the CMB shift parameter, the BAO's, the growth rate for structure formation (see the next section), and the BBN and CMB anisotropy bounds. Contour lines for $\nu_{\text{eff}} = 1 - \xi$ are shown in Figure 2 for model G2 at fixed $\xi^l = 1$. The χ^2 functions associated to SN Ia distance modulus $\mu(z)$, the BAO A -parameter, and the CMB shift parameter can be found in Gómez-Valent et al. (2015). Therein, one can also find the corresponding references of the data sets that we have used in the present analysis.

4. LINEAR STRUCTURE FORMATION

Finally, we take into consideration the data on the linear structure formation. For the G1 and G2 models the calculation of $\delta_m = \delta \rho_m / \rho_m$ is significantly more complicated than in the Λ CDM case and follows from applying linear perturbation theory to Einstein's field equations and Bianchi identity (5)

Table 1
Best-fit Values for G1-type Models

Model	$ \frac{\Delta G}{G_0} $ (BBN,CMB), $\text{Om}h^2$	Ω_m	$\bar{\Omega}_m$ (All Data)	ν	$\bar{\nu}$	σ_8	$\bar{\sigma}_8$	χ^2/dof	$\bar{\chi}^2/\text{dof}$	AIC	$\bar{\text{AIC}}$
Λ CDM	..., Yes	$0.278^{+0.005}_{-0.004}$	0.276 ± 0.004	0.815	0.815	828.84/1010	828.69/1010	830.84	830.69
G1	(10%,5%), Yes	0.278 ± 0.006	0.275 ± 0.004	$0.0015^{+0.0017}_{-0.0015}$	$0.0021^{+0.0014}_{-0.0016}$	0.797	0.784	822.82/1009	821.97/1009	826.82	825.97
Λ CDM	..., No	0.292 ± 0.008	0.286 ± 0.007	0.815	0.815	583.38/604	582.74/604	585.38	584.74
G1	(10%,5%), No	0.290 ± 0.011	0.281 ± 0.005	$0.0008^{+0.0016}_{-0.0015}$	0.0015 ± 0.0014	0.795	0.771	577.62/603	575.70/603	581.62	579.70
Λ CDM*	..., Yes*	0.297 ± 0.006	0.293 ± 0.006	0.815	0.815	806.68/982	806.17/982	808.68	808.17
G1*	(10%,5%), Yes*	0.296 ± 0.009	0.287 ± 0.004	0.0006 ± 0.0015	$0.0012^{+0.0014}_{-0.0013}$	0.803	0.770	802.66/981	799.15/981	806.66	803.15

Note. The best-fitting values for the G1-type models and their statistical significance (χ^2 -test and Akaike information criterion AIC, see the text). All quantities with a bar involve a fit to the total input data, i.e., the expansion history ($\text{Om}h^2$ +BAO+SN Ia), CMB shift parameter, the indicated constraints on the value of $\Delta G/G_0$ at BBN and at recombination, as well as the linear growth data. Those without bars correspond to a fit in which we use all data but exclude the growth data points from the fitting procedure. “Yes” or “No” indicates whether or not $\text{Om}h^2$ enters the fit. The starred scenarios correspond to removing the high-redshift point $z = 2.34$ from $\text{Om}h^2$ (see the text). The quoted number of degrees of freedom (dof) is equal to the number of data points minus the number of independent fitting parameters. The fitting parameter ν includes all data.

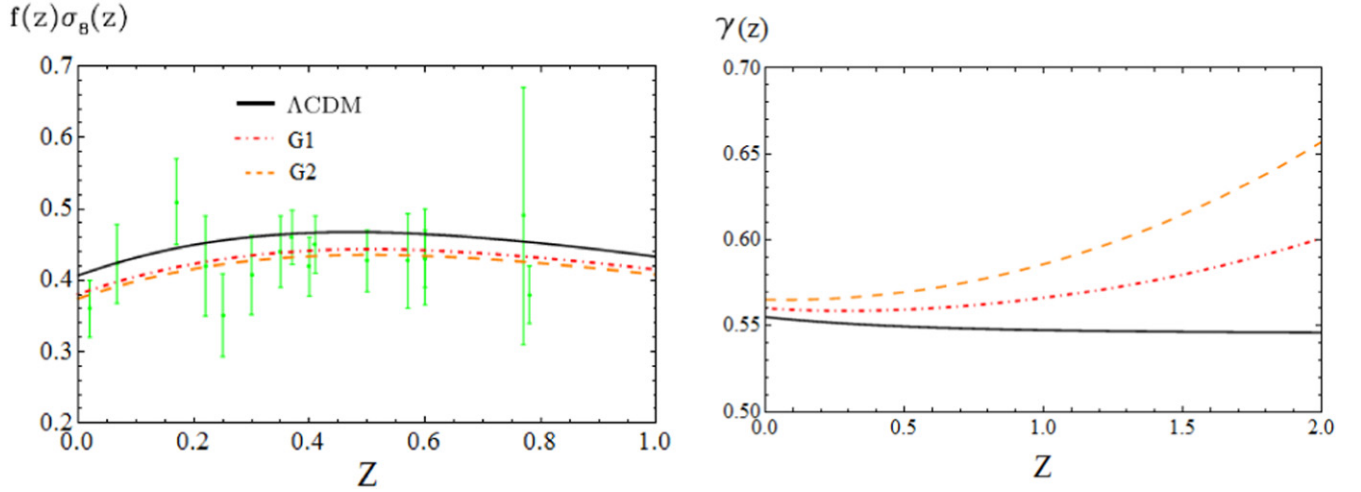


Figure 3. Left: comparison of the observed data with error bars (in green) and the theoretical evolution of the weighted growth rate of clustering $f(z)\sigma_8(z)$ for each dynamical vacuum model and the Λ CDM. Right: the corresponding evolution of the linear growth index $\gamma(z)$.

(Grande et al. 2010, 2011). The final result reads:³

$$\delta_m''' + \frac{\delta_m''}{2a}(16 - 9\Omega_m) + \frac{3\delta_m'}{2a^2}(8 - 11\Omega_m + 3\Omega_m^2 - a\Omega_m') = 0, \quad (15)$$

with $\Omega_m(a) = 8\pi G(a)\rho_m(a)/3H^2(a)$. Note that the (ν, α) model-dependence is encoded in $G(a)$ and $H(a)$ —see Equations (6), (7), and (8). To solve the above equation (numerically) we have to fix the initial conditions for δ_m, δ_m' , and δ_m'' . We take due account of the fact that for these models at small a (when non-relativistic matter dominates over the vacuum) we have $\delta_m(a) = a^s$, where $s = 3\xi - 2 = 1 - 3\nu_{\text{eff}}$. If $\xi = 1$ ($\nu_{\text{eff}} = 0$), then $\delta_m(a) \sim a$ and we recover the Λ CDM behavior. Thus, the initial conditions set at a high redshift $z_i = (1 - a_i)/a_i$, say $z_i = 100$ (or at any higher value), are as follows. For the growth factor we have $\delta_m(a_i) = a_i^s$, and for its derivatives: $\delta_m'(a_i) = sa_i^{s-1}$, $\delta_m''(a_i) = s(s-1)a_i^{s-2}$.

In practice we investigate the agreement with the structure formation data by comparing the theoretical linear growth prediction $f(z) = -(1+z)d \ln \delta_m/dz$ and the growth rate index $\gamma(z)$ with the available growth data—following Gómez-Valent et al. (2015 and references therein) and Gómez-Valent & Solà (2015). Recall that γ is defined through $f(z) \simeq \Omega_m(z)^{\gamma(z)}$, and one typically expects $\gamma(0) = 0.56 \pm 0.05$ for Λ CDM-like models (Pouri et al. 2014). A most convenient related quantity is the weighted growth rate $f(z)\sigma_8(z)$ (see Song & Percival 2009), where $\sigma_8(z)$ is the rms mass fluctuation amplitude on scales of $R_8 = 8 h^{-1}$

Mpc at redshift z . The latter is computed from

$$\sigma_8(z) = \sigma_{8,\Lambda} \frac{\delta_m(z)}{\delta_m^\Lambda(0)} \left[\frac{\int_0^\infty k^{n_s+2} T^2(\Omega_m, k) W^2(kR_8) dk}{\int_0^\infty k^{n_s+2} T^2(\Omega_{m,\Lambda}, k) W^2(kR_8) dk} \right]^{1/2}, \quad (16)$$

with W being a top-hat smoothing function (see, e.g., Gómez-Valent et al. 2015 for details) and $T(\Omega_m, k)$ the transfer function, which we take from Bardeen et al. (1986). The values of $\sigma_8 \equiv \sigma_8(0)$ for the various models are collected in Table 1, and in Figure 3 we plot $f(z)\sigma_8(z)$ and $\gamma(z)$ for each.

The joint likelihood analysis is performed on the set of $\text{Om}h^2 + \text{BAO} + \text{SN Ia} + \text{CMB}$, BBN and linear growth data, involving one (Ω_m) or two ($\Omega_m, \nu_{\text{eff}}$) independently adjusted parameters depending on the model. For the Λ CDM we have one parameter ($n_p = 1$) and for G1 and G2 we have $n_p = 2$. Recall that for G2 we have fixed $\xi' = 1$.

5. DISCUSSION

The main results of this work are synthesized in Tables 1–2 and Figures 1–3. In particular, from Figure 2 we see that the model parameter ν_{eff} for G2 is clearly projected onto the positive region, which encompasses most of the 3σ range. Remarkably, the χ^2 -value of the overall fit is smaller than that of Λ CDM for both G1 and G2 (see Tables 1–2). To better assess the distinctive quality of the fits we apply the well known Akaike Information Criterion (AIC; Akaike 1974; Burnham & Anderson 2002), which requires the condition $N_{\text{tot}}/n_p > 40$ (amply satisfied in our case). It is defined, for Gaussian errors, as follows: $\text{AIC} = -2 \ln \mathcal{L}_{\text{max}} + 2n_p = \chi_{\text{min}}^2 + 2n_p$, where \mathcal{L}_{max} (resp. χ_{min}^2) is the maximum (resp. minimum) of the likelihood (resp. χ^2) function. To test the effectiveness of models M_i and M_j , one considers the pairwise difference $(\Delta \text{AIC})_{ij} = (\text{AIC})_i - (\text{AIC})_j$. The larger the value of $\Delta_{ij} \equiv |\Delta(\text{AIC})_{ij}|$, the higher the evidence against the model with larger value of AIC, with $\Delta_{ij} \geq 2$ indicating a positive such evidence and $\Delta_{ij} \geq 6$ denoting significant such evidence.

³ The third-order feature of this equation is characteristic of the coupled systems of matter and DE perturbations for cosmologies with matter conservation, after eliminating the perturbations in the DE in favor of a single higher order equation for the matter part (see Gómez-Valent et al. 2015 for details). For $\Lambda = \text{const.}$, Equation (15) boils down to the (derivative of the) second order one of the Λ CDM.

Table 2
Best-fit Values for G2-type Models

Model	$ \frac{\Delta G}{G_0} $ (CMB), Omh^2	Ω_m	Ω_m (all data)	ν_{eff}	$\bar{\nu}_{\text{eff}}$	σ_8	$\bar{\sigma}_8$	χ^2/dof	$\bar{\chi}^2/\text{dof}$	AIC	$\bar{\text{AIC}}$
Λ CDM	..., Yes	$0.278^{+0.005}_{-0.004}$	0.276 ± 0.004	0.815	0.815	828.84/1009	828.69/1009	830.84	830.69
G2	5%, Yes	0.278 ± 0.006	0.277 ± 0.004	$0.0038^{+0.0025}_{-0.0023}$	$0.0043^{+0.0018}_{-0.0020}$	0.774	0.773	817.17/1008	817.26/1008	821.17	821.26
Λ CDM	..., No	0.292 ± 0.008	0.286 ± 0.007	0.815	0.815	583.38/603	582.74/603	585.38	584.74
G2	5%, No	0.287 ± 0.011	0.283 ± 0.005	$0.0025^{+0.0026}_{-0.0025}$	$0.0030^{+0.0021}_{-0.0018}$	0.763	0.767	572.68/602	572.99/602	576.68	576.99
Λ CDM*	..., Yes*	0.297 ± 0.006	0.293 ± 0.006	0.815	0.815	806.68/981	806.17/981	808.68	808.17
G2*	5%, Yes*	0.295 ± 0.009	0.289 ± 0.005	$0.0015^{+0.0026}_{-0.0025}$	$0.0028^{+0.0018}_{-0.0021}$	0.789	0.765	798.85/980	797.05/980	802.85	801.05

Note. As in Table 1, but for G2 models with $\xi' = 1$ so as to maximally preserve the BBN bound (see the text). The effective G2 model fitting parameter in this case is $\nu_{\text{eff}} = \nu/4$. The constraint on $|\Delta G/G_0|$ from CMB anisotropies at recombination is explicitly indicated.

From Tables 1–2 we see that when we compare the fit quality of models $i = G1, G2$ with that of $j = \Lambda\text{CDM}$, in a situation when we take all the data for the fit optimization, we find $\bar{\Delta}_{ij} \equiv \Delta\text{AIC} \gtrsim 9.43$ for G2 and 4.72 for G1, suggesting significant evidence in favor of these models (especially G2) against the ΛCDM —the evidence ratio (Akaike 1974) being $\text{ER} = e^{\Delta_{ij}/2} \gtrsim 111.6$ for G2 and 10.6 for G1. Also worth noting is the result of the fit when we exclude the growth data from the fitting procedure but still add their contribution to the total χ^2 . This fit is, of course, less optimized, but allows us to risk a prediction for the linear growth and hence to test the level of agreement with these data points (see Figure 3). It turns out that the corresponding AIC pairwise difference with the ΛCDM are similar as before (see Tables 1–2). Therefore, the ΛCDM appears significantly disfavored versus the dynamical vacuum models, especially in front of G2, according to the AIC. Let us mention that if we remove all of the $H(z)$ data points from our analysis the fit quality weakens, but it still gives a better fit than the ΛCDM (see the third and fourth rows of Tables 1 and 2). If, however, we keep these data points but remove *only* the high-redshift point $z = 2.34$ (Delubac et al. 2015), the outcome is not dramatically different from the previous situation (confer the starred scenarios in Tables 1 and 2), as in both cases the significance of $\nu_{\text{eff}} \neq 0$ is still close to $\sim 2\sigma$ with $\Delta_{ij} > 7$ for G2 (hence still strongly favored, with $\text{ER} > 33$). In this sense the high z point may not be so crucial for claiming hints in favor of dynamical vacuum, as the hints themselves seem to emerge more as an overall effect of the data. While we are awaiting for new measurements of the Hubble parameter at high redshift to better assess their real impact, we have checked that if we add to our analysis the points $z = 2.30$ (Busca et al. 2013) and $z = 2.36$ (Font-Ribera et al. 2014), not included in either Sahni et al. (2014) or Ding et al. (2015), our conclusions remain unchanged. Ditto if using the three high z points only.

To summarize, our study singles out a general class of vacuum models, whose dynamical behavior challenges the overall fit quality of the rigid Λ -term inherent to the concordance ΛCDM model. From the data on expansion, structure formation, and BBN and CMB observables we conclude that the ΛCDM model is currently disfavored at the $\sim 3\sigma$ level as compared to the best dynamical ones.

We thank the anonymous referee for the thorough report on our work and for very useful suggestions to improve our analysis. J.S. has been supported in part by MICINN, CPAN, and Generalitat de Catalunya; A.G.V. acknowledges support by APIF grant of the U. Barcelona.

REFERENCES

- Ade, P. A. R., Aghanim, N., Arnaud, M., et al. (Planck Collaboration) 2015, arXiv:1502.01589
- Akaike, H. 1974, *ITAC*, **19**, 716
- Bardeen, J. M., Bond, J. R., Kaiser, N., & Szalay, A. S. 1986, *ApJ*, **304**, 15
- Basilakos, S., & Solà, J. 2014, *MNRAS*, **437**, 3331
- Burnham, K. P., & Anderson 2002, *Model Selection and Multimodel Inference* (New York: Springer)
- Busca, N. G., Delubac, T., Rich, J., et al. 2013, *A&A*, **552**, A96
- Chiba, T. 2011, *PThPh*, **126**, 993
- Delubac, T., Bautista, J. E., Busca, N. G., et al. 2015, *A&A*, **574**, A59
- Ding, X., Biesiada, M., Cao, S., Li, Z., & Zhu, Z.-H. 2015, *ApJL*, **803**, L22
- Farooq, O., & Ratra, B. 2013, *ApJL*, **766**, L7
- Font-Ribera, A., Kirkby, D., Busca, N., et al. 2014, *JCAP*, **05**, 027
- Gómez-Valent, A., Karimkhani, E., & Solà, J. 2015, arXiv:1509.03298
- Gómez-Valent, A., & Solà, J. 2015, *MNRAS*, **448**, 2810
- Gómez-Valent, A., Solà, J., & Basilakos, S. 2015, *JCAP*, **01**, 004
- Grande, J., Solà, J., Basilakos, S., & Plionis, M. 2011, *JCAP*, **08**, 007
- Grande, J., Solà, J., Fabris, J. C., & Shapiro, I. L. 2010, *CQGr*, **27**, 105004
- Lima, J. A. S., Basilakos, S., & Solà, J. 2013, *MNRAS*, **431**, 923
- Lima, J. A. S., Basilakos, S., & Solà, J. 2015, *GRGr*, **47**, 40
- Nagata, R., Chiba, T., & Sugiyama, N. 2004, *PhRvD*, **69**, 083512
- Padmanabhan, T. 2003, *PhR*, **380**, 235
- Peebles, P. J. E., & Ratra, B. 2003, *RvMP*, **75**, 559
- Perlmutter, S., Aldering, G., Goldhaber, G., et al. 1999, *ApJ*, **517**, 565
- Pouri, A., Basilakos, S., & Plionis, M. 2014, *JCAP*, **08**, 042
- Riess, A. G., Filippenko, A. V., Challis, P., et al. 1998, *AJ*, **116**, 1009
- Sahni, V., Shafieloo, A., & Starobinsky, A. A. 2014, *ApJL*, **793**, L40
- Sahni, V., & Starobinsky, A. A. 2000, *IJMPA*, **9**, 373
- Shafieloo, A., Alam, U., Sahni, V., & Starobinsky, A. A. 2006, *MNRAS*, **366**, 1081
- Shapiro, I. L., & Solà, J. 2002, *JHEP*, **02**, 006
- Shapiro, I. L., & Solà, J. 2009, *PhLB*, **682**, 105
- Solà, J. 2008, *JPhA*, **41**, 164066
- Solà, J. 2013, *JPhCS*, **453**, 012015
- Solà, J. 2015, *IJMPD*, in press (arXiv:1505.05863)
- Solà, J., & Gómez-Valent, A. 2015, *IJMPD*, **24**, 1541003
- Solà, J., & Stefancic, H. 2005, *PhLB*, **624**, 147
- Solà, J., & Stefancic, H. 2006, *MPLA*, **21**, 479
- Song, Y.-S., & Percival, W. J. 2009, *JCAP*, **10**, 004
- Sugiura, N. 1978, *Commun. Stat. A, Theory Methods*, **7**, 13
- Uzan, J.-P. 2011, *LRR*, **14**, 2
- Weinberg, S. 1989, *RvMP*, **61**, 1